D-axis stator current control methods applied to PMSG-based wind energy systems: A comparative study

Tuan Ngoc Anh Nguyen
Faculty of Electrical Engineering
Industrial University of Ho Chi Minh City
Ho Chi Minh City, Vietnam
nnatuan@gmail.com

Duy Cong Pham*
Faculty of Electrical Engineering
Industrial University of Ho Chi Minh City
Ho Chi Minh City, Vietnam
dph@iuh.edu.vn

Cong-Thanh Pham*
Faculty of Electrical and Electronics Engineering
Ho Chi Minh City University of Food Industry
Ho Chi Minh City, Vietnam.
phamcongthanh1978@gmail.com

Nguyen Huu Chan Thanh
Faculty of Electrical and Electronics Engineering
Ho Chi Minh City University of Transport
Ho Chi Minh City, Vietnam
chanthanhnguyen@gmail.com

Abstract: - A comparative study of three d-axis stator current control methods for machine side converter in permanent magnet synchronous generator based on wind energy systems is proposed in this paper. Firstly, the zero d-axis stator current (ZDC) control method is performed by setting set the d-axis component of the stator current to zero. Secondly, the unity power factor (UPF) control method is designed to set the angle between stator current vector and stator voltage vector to zero. Thirdly, the constant stator flux-linkage (CSFL) control method is designed to regulate the stator flux-linkage, making it equal to the permanent magnet flux linkage. Finally, the performance of the three control methods are evaluated and compared based on some key parameters, which are the d-axis current, q-axis current, stator flux, active power, reactive power and apparent power, power factor under the same operating conditions. The feasibility and effectiveness of the three d-axis stator current control methods are demonstrated through Matlab simulations.

Key-Words: - Permanent magnet synchronous generator (PMSG), wind energy systems (WES), wind energy conversion system (WECS), zero d-axis stator current (ZDC) control, unity power factor (UPF) control, constant stator flux-linkage (CSFL) control.

1 Introduction

With the negative impacts of global warming and harmful effects of fossil-fuel emissions, electricity production from renewable energy sources has attracted a lot of attention in recent years [1]. Among all the renewable energy sources, wind energy is gaining interest from both industrial [1] and academic fields [2,3], because of its competitiveness against conventional sources of energy, in terms of technological advancements, cost reduction, and government incentives and support programs [1].

The wind energy conversion system (WECS) includes wind electric generators, power converter, and transformer [2]. The wind electric generator such as the squirrel-cage induction generator (SCIG), wound rotor induction generator (WRIG), doubly-fed induction generator (DFIG), wound rotor synchronous generator (WRSG), and Permanent magnet synchronous generator (PMSG) are used to convert rotational mechanical-energy into electric-energy, which have been researched and developed over the last three decades [1]. Each of them has different advantages and limitations. Among variable-speed wind generators, the PMSGs have received increasing attention because of high-efficiency, high-reliability, and gearless operation [4]. Until now, a PMSG wind turbine using a full-scale back-to-back (BTB) connected two-level voltage-source converter (2L-VSC), including machine side converter (MSC) and grid-side converter (GSC) are realized by low-voltage insulated gate bipolar transistors (IGBTs) arranged in matrix form. The GSC is designed with higher mega volt-ampere capacity than the MSC. The DC-link provides decoupling between the PMSG and grid; The advantages of it is simple structure, low cost because of the mass production and the transients in the PMSG do not appear on the grid side as illustrated in Fig.1. The main function of the MSC is to completely regulate the generator in terms of speed, active power, power factor, and electromagnetic torque, while the GSC is to regulate the dc-link voltage and the grid reactive power [5,6]. The control of a WECS is becoming more significant, especially when using the electrical generator based on PMSG. With many different aims, such as improving the performance, efficiency, and reliability, the PMSG is controlled through many modeling methods such as mathematical modeling, dynamic response analysis, the control of PMSG-based wind turbines control operating with an alternative control structure in power control mode [7] or modeling and simulation of multi-scale transients for PMSG-based wind power systems [8] or small-signal-stability-analysis-for-different-types-of-PMSGs connected to the grid [9] or stability analysis and improvements for variable speed multipole PMSG-based WECS [10] and an unified power control for PMSG-based WECS operating under different grid conditions [11]. However, the main drawback of three control method is that it depends highly on the design modeling and parameters, such as the stator and rotor resistances, inductances and complex calculation. In order to improve the quality of the electrical power produced by wind generators, a comparative study of classical vector, first-order sliding-mode and high-order sliding-mode is carried out, with control for a grid-connected variable-speed WECS [12] and an enhancement low-voltage ride through capability of permanent magnet synchronous generator-based wind turbines using interval type-2 fuzzy control [13] or pitch angle control for grid-connected variable-speed wind turbine system using fuzzy logic [14]. These control methods have good characteristics, such as reliability, fast dynamic response, insensitivity against disturbances, and wind velocity fluctuations. Nevertheless, these strategies still have some drawbacks related to the chattering problem. The predictive techniques [15] was proposed in order to solve this issue. However, these strategies still have some disadvantages related to the hysteresis controllers since it can cause torque and current distortions, as well as limiting the steady-state accuracy.

Alternatively, the three control methods, namely, zero d-axis stator current (ZDC) control, unity power factor (UPF) control and constant stator flux-linkage (CSFL) control, presented in [16] which applied to control for the PMSM. The ZDC control is widely used in the industry. Its own merit is easy perform and its own demerits is the low power factor. The UPF control optimizes the system’s apparent power (volt–ampere requirement) by maintaining the power factor at unity, the main drawback of it is shown to yield a very low torque per unit current ratio. The CSFL control method limits the air gap flux linkages to any set or desired flux linkages. This control method, therefore, leads to a seamless flux-weakening method in the PMSM drive and is to be noted but up to now no paper presents the CSFL control method to apply for PMSG. The ZDC control and UPF control [17] are compared and established an optimized control for the generator-side converter of the Z-source applied to PMSG. The ZDC control [18] is combined with the hysteresis controller to control the current for the machine side converter to find the maximum power point, however, it requires the algorithm modeling and complex calculation. The scope of this paper is to fill the gap in the current literature by three d-axis stator current control methods for MSC of PMSG connected to the grid via VSC.

This paper is organized as follows. Model of PMSG is luxurious books by WSEAS Press. Thank you for your cooperation and contribution. We are looking forward to seeing you at the Conference. stator current control methods for machine side converter are presented in detail. Simulink verifications of a PMSG wind system with the proposed solutions are illustrated in Section 4. Finally, Section 5 concludes this paper.

speed increases, the maintenance of the nominal power is obtained with the control of the blade position (pitch control). There are different ways to adhere to the maximum power characteristic (so-called

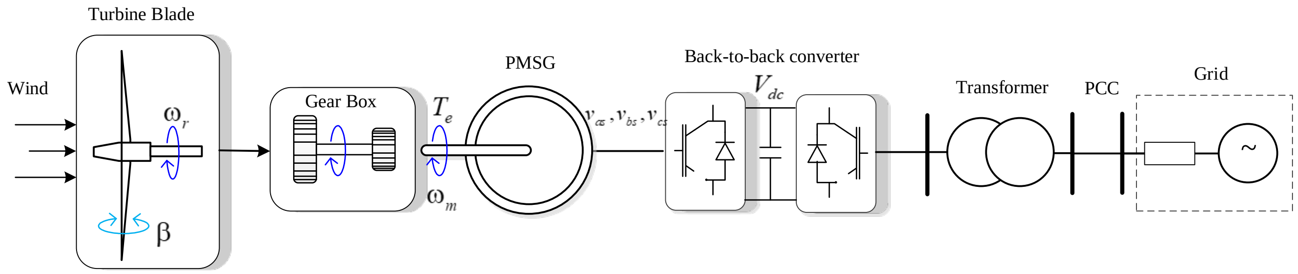

Fig.1 Permanent magnet synchronous generator wind energy system used for study

maximum power point tracking—MPPT), including the following:

- To control the WG rotating speed so that it corresponds to the value αm with the present wind speed.
- To load WG with the power P_{mmax} under present wind speed.
- To set WG power (or torque) so that it is equal to the maximum possible WG power under present WG rotating speed.

$$P_{m\max} = \left(\frac{K_p C_{p\max} R^3}{\alpha_m}\right)\omega_m^{\ 3} \quad (5)$$

2 Permanent magnet synchronous generator wind turbine systems

2.1 Wind turbine aerodynamic model

The key function of a wind turbine is to extract kinetic energy from different wind velocities and converts it into mechanical energy. Thus, wind turbine power production depends on the interaction between the rotor and the wind. The mechanical output power of the turbine and the turbine torque are given by the following equation [2].

$$P_m = \frac{1}{2}\rho A C_p(\alpha,\beta) v_{wind}^3 = K_p C_p(\alpha,\beta) v_{wind}^3 \quad (1)$$

$$T_m = K_p R v_{wind}^2 C_p(\alpha,\beta)/\alpha = K_m v_{wind}^2 C_m(\alpha,\beta) \quad (2)$$

where ρ is the air density (kg/m3); A is the area swept by the blades (m2) and equal to πR^2, R is the blade length; v_{wind} is the wind speed (m/s); C_p is the power coefficient of the turbine, which is function of the tip speed ratio α and the blade pitch angle β (degree) and $K_m = K_p R$; $C_m = C_p/\alpha$ .The definitions of tip speed ratio and C_p are given as (3) and (4); where R, ω_m represent the turbine rotor radius and mechanical velocity, respectively.

$$\alpha = \frac{\omega_m R}{v_{wind}} \quad (3)$$

$$C_p(\alpha) = c_1\left(\frac{c_2}{\alpha_i} - c_3\beta - c_4\right)e^{\left(-\frac{c_5}{\alpha_i}\right)} + c_6\alpha \quad (4)$$

Where c_1= 0.5176, c_2=116, c_3= 0.4, c_4= 5, c_5= 21, c_6= 0.0068 and $\alpha_i = \left(\frac{1}{\alpha + 0.08\beta} - \frac{0.035}{1+\beta^3}\right)^{-1}$ When the wind

2.2 Dynamic modeling of permanent magnet synchronous generators

This section presents dynamic modeling of the PMSG. Considering that the PMSG used in this paper is a surface-mounted machine, it can be assumed that $L_s = L_d = L_q$. The PMSG model is considered under the following assumptions.

- The spatial distribution of stator winding is sinusoidal.
- The core loss is neglected.
- The saturation is neglected.
- The damping effect is neglected.

Thus, the equations of PMSG in the rotor *dq* reference frame are given as follows [2].

$$u_{ds} = R_s i_{ds} + \frac{d\lambda_{ds}}{dt} - \omega_r \lambda_s \quad (6)$$

$$u_{qs} = R_s i_{qs} + \frac{d\lambda_{qs}}{dt} + \omega_r \lambda_s \quad (7)$$

$$\lambda_{ds} = L_s i_{ds} + \lambda_r \quad (8)$$

$$\lambda_{qs} = L_s i_{qs} \tag{9}$$

$$T_e = \frac{3}{2}\rho i_{qs}\lambda_r \tag{10}$$

$$T_e - T_L = J\frac{d\omega_r}{dt} + B\omega_r \tag{11}$$

where uds and uqs are the d-axis and q-axis stator terminal voltages, respectively; ids and iqs are respectively the d-axis and q-axis stator current, Rs is the resistance of the stator windings; ωr (= pωt) is the electrical angular velocity of the rotor; p is the number of pole pairs; λr is the amplitude of the flux linkage; λds and λ_{qs} are the *d*-axis and *q*-axis flux-linkages; T_e is the torque; T_L is the load torque; *J* is the inertial; *B* is the friction coefficient.

In steady-state condition, the equations of PMSG are given by:

$$u_{ds} = R_s i_{ds} - \omega_r L_s i_{qs} \tag{12}$$

$$u_{qs} = R_s i_{qs} + \omega_r L_s i_{ds} + \omega_r \lambda_r \tag{13}$$

The active and reactive powers at generator terminals based on the rotating reference frame, given as

$$P = \frac{3}{2}(u_{ds}i_{ds} + u_{qs}i_{qs}) \tag{14}$$

$$Q = \frac{3}{2}(u_{ds}i_{qs} - u_{qs}i_{ds}) \tag{15}$$

The apparent power is given by

$$S = \sqrt{P+Q} \tag{16}$$

3 *d*-axis stator current control methods

For implementing a control method, factors such as cost, ease of implementation, and waveform quality must be considered in detail. Specially, assessment of generator performances is based on generator efficiency, generator power factor, and generator stator current. In this section, three control methods, which are ZDC control, UPF control, CSFL control, are investigated in Fig.2.

3.1 ZDC

In order to implement this control method (i_{ds} = 0), the *d*-axis component of the stator current i_{ds} is set to zero. Only the quadrature-axis stator current i_{qs} produces torque in a generator. In other words, this control method keeps the torque angle (Θ_i) (angle between stator current vector and permanent magnet flux vector) at constant value of 90°.

3.2 UPF

Under this control method, the stator current vector and stator voltage vector are in the same direction. Hence, power factor angle becomes zero. The overall volt–ampere of the generator side converter would contribute to the active power transfer and thereby reduce the power rating of the generator-side converter configuration. This would lead to a smaller size and hence reduce the cost of the power circuit, which is one of the significant considerations for megawatt-level wind energy conversion system design without additional hardware.

Under UPF operating condition, the reactive power should equal to zero, it means

$$u_{ds}i_{qs} - u_{qs}i_{ds} = 0 \tag{17}$$

Substituting equation (12) and equation (13) into equation (17), then

$$L_s i_{ds}^2 + \lambda_r i_{ds} + L_s i_{qs}^2 = 0 \tag{18}$$

$$i_{ds}^* = \begin{cases} -\frac{i_m}{2} + \sqrt{(\frac{i_m}{2})^2 - (i_{qs}^*)^2} & valid \\ \frac{i_m}{2} + \sqrt{(\frac{i_m}{2})^2 - (i_{qs}^*)^2} & not \quad valid \end{cases}$$

where $i_m = \frac{\lambda_r}{L_s}$ is the virtual current.

According to the Park transformation, in case generating i_{qs} and i_{ds} are negative. Therefore, from equation (18), the relation between *d*- and q-axis stator currents for UPF condition is

$$i_{ds}^* = -\frac{i_m}{2} + \sqrt{(\frac{i_m}{2})^2 - (i_{qs}^*)^2} \tag{19}$$

It should be noted that when the equation (18) condition is satisfied, the PMSG operates with UPF.

3.3 CSFL

The constant stator flux-linkage is used to overcome the problem of increasing stator flux linkage as the torque reference value is increased, which can lead to saturation of the stator yoke. The main feature of this method is good steady state performances, high machine power factor, and comparatively small required power converter capacity. In order to implement this control method, the magnitude of the stator flux vector is maintained constant and equal to the permanent magnet flux.

$$|\lambda_s| = \sqrt{(L_s i_{ds} + \lambda_r)^2 + (L_s i_{qs})^2} = \lambda_r \tag{20}$$

$$(i_{ds} + \frac{\lambda_r}{L_s})^2 + (i_{qs})^2 = (\frac{\lambda_r}{L_s})^2$$

$$(i_{ds} + i_m)^2 + (i_{qs})^2 = (i_m)^2 \tag{21}$$

From Equation (20), the relation between *d*- and *q*-axis stator currents for CSFL condition is

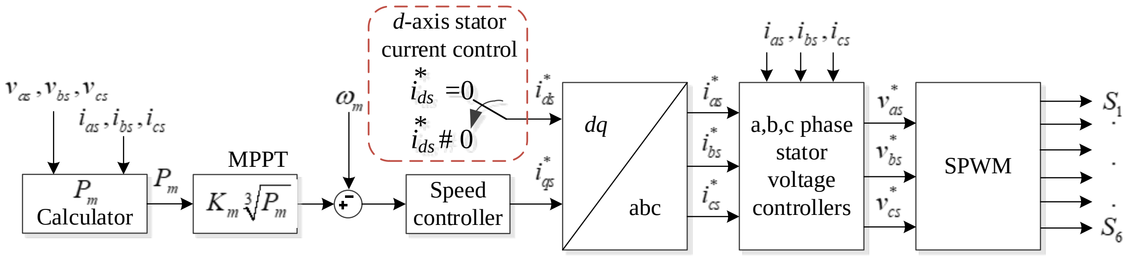

Fig.2. Block diagram of proposed *d*-axis stator current control methods.

$$i_{ds}^* = -i_m + \sqrt{(i_m)^2 - (i_{qs}^*)^2}$$

It should be noted that when equation (21) is satisfied, the PMSG operates with CSFL. Equation (21) also shows that the generator generates a negative current command for the CSFL operating condition.

4 Simulation results

In order to evaluate the advantages and drawbacks of the proposed three stator current control methods, several sets of simulations are conducted using Matlab. The simulation results in Matlab show the waveforms of active and reactive power, power factor and the current in generator side. The effectiveness of the ZDC control method, UPF control method and CSFL control method of the machine side converter is examined under different operating conditions. The parameters of the PMSG and turbine are given in Tables 1. and 2.

TABLE 1: GENERATOR PARAMETERS USED IN SIMULATION

Description	***Parameter***	***Value***
Transparent power	S_n	2.2MW
Nominal current	I_n	2606A
Nominal Voltage	u_n	690V
dc-link voltage	u_{dc}	1200 V
Nominal rotating speed	ω_m	2.355 rad/s
Number of poles	Z_p	26
Nominal moment	T_e	934.2 kNm
Viscous damping	B	0.004 Nms
Stator phase resistance	R_s	0.0008 Ω
Stator phase inductance	L_s	0.00157 H
Flux linkage	λ_r	9.18 Wb
Inertia of rotor	J	0.0000005 kg.m2

In this case, the response of the three stator current control methods is tested under wind speed variation. For this study, the wind speed is assumed to be 10 m/s and then increased to 12 m/s at t = 15s and then decreased to 7 m/s at t = 40s as illustrated in Fig.5a. In turn, active power and the *q*-axis stator current in three control methods are approximately of the same value as wind speed variation.

TABLE 2: GENERATOR PARAMETERS USED IN SIMULATION

Description	***Parameter***	***Value***
Rated power	P_n	2MW
Nominal rotating speed	ω_n	2.355 rad/s
Inertia of rotor	J	0.00025034 kg.m2
Blades length	R	37.1 m
Base wind speed	v_{wind}	6-12m/s

The *d*-axis stator current is assumed to be fixed at zero value to extract maximum torque/power and avoid demagnetization of the permanent magnet. The simulation results of the *d*-*q*-axis stator current (i_{dZDC}, i_{dUPF}, i_{dCSFL}, i_{qZDC}, i_{qUPF}, i_{qCSFL}) in three control methods are illustrated in Fig.5 b, c. The results show that the UPF control method has the highest amplitude value in the waveforms of *d*-axis stator current, during the ZDC control method has zero value in the waveforms of *d*-axis stator current. Therefore, the UPF control method will have to choose the wire with large cross section for machine side converter and this reason increase the costs. It can be seen that the *q*-axis stator current in three control methods are approximately of the same value ($i_{qZDC} = i_{qUPF} = i_{qCSFL}$). The simulation results of stator flux (λ_{ZDC}, λ_{UPF}, λ_{CSFL}) in three control methods are illustrated in Fig.5. d. It shows that, the stator flux of ZDC control method has the highest value, the stator flux of UPF control method has the lowest value with various speed. It can be seen that the stator flux of CSFL control method has no changed.

The simulation results show the waveforms of active power, reactive power, apparent power, power factor and stator current respectively. Fig. 6 shows the active power (P_{ZDC}, P_{UPF}, P_{CSFL}) and reactive power (Q_{ZDC}, Q_{UPF}, Q_{CSFL}) of three control methods, in that the active power is approximately the same value ($P_{ZDC} = P_{UPF} = P_{CSFL}$) because of according to (10) torque or active power are proportional with q-axis stator current (as mentioned above, the Simulink results in Fig. 5.c shows that the *q*-axis stator current in three control methods are of the same value). Furthermore, the reactive power in UPF control method is zero at all times, the highest value is reactive power in ZDC control method. It can be seen that in Fig.7. There are three case of apparent power (S_{ZDC}, S_{UPF}, S_{CSFL}). Firstly, the wind speed is high (12 m/s) the ZDC control method has the highest value in the waveforms of apparent power. Therefore, the ZDC control method will have to impact on IGBT and this reason increase the costs, while the UPF control method has the lowest oscillation in the waveforms of apparent power. Secondly, the apparent power in ZDC control method has the highest value but the UPF and CSFL control method is approximately the same value at the wind speed is from 8 m/s to 11 m/s. Thirdly, the apparent power in three control methods is approximately the same value at the wind speed is low (under 8 m/s). According to Fig.8. the power factor in UPF control method has the highest value (θ_{UPF}) and the power factor in CSFL control method (θ_{CSFL}) has the middle value and power factor in ZDC control method (θ_{ZDC}) has the lowest value. The stator current in three control methods (i_{sZDC}, i_{sUPF}, i_{sCSFL}). is illustrated in Fig.9. It shows that there are two case. Firstly, the wind speed is from 8m/s to 12 m/s. The stator current of UPF control method is the highest value so that the UPF control method will have to choose the wire with large cross section for machine side converter and this reason increase the costs and the ZDC control method is the lowest value. Secondly, the stator current in three control methods is approximately the same value as the wind speed is low (under 8 m/s).

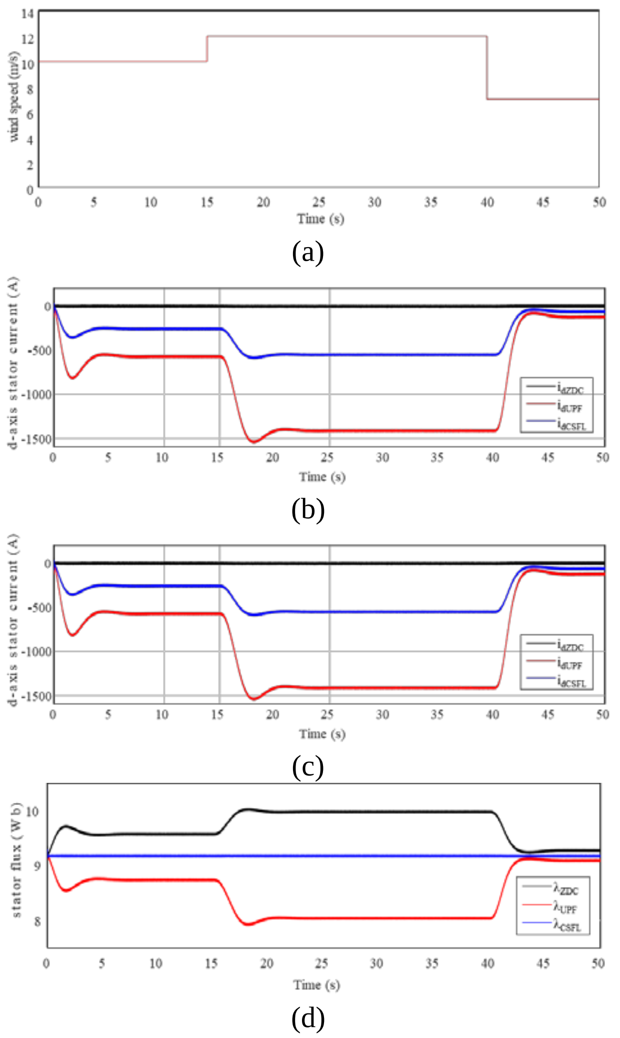

Fig.5 Simulation results regarding the time-domain waveforms: (a) wind speed; (b) *d*-axis stator current in three control methods; (c) *q*-axis stator current in three control methods; (d) stator flux in three control methods.

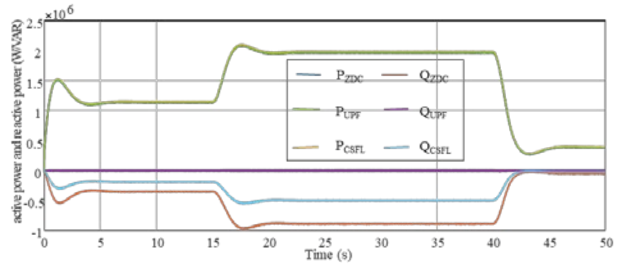

Fig.6 Simulation results regarding the time-domain waveforms of active- and reactive power in three control methods.

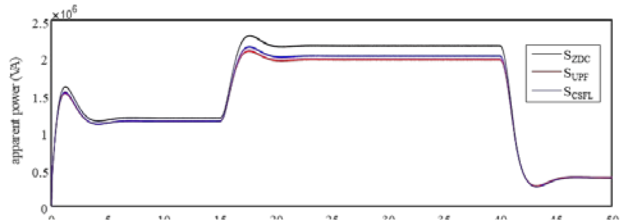

Fig.7 Simulation results regarding the time-domain waveforms of apparent power in three control methods.

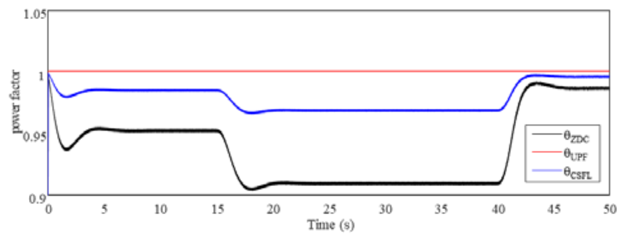

Fig.8 Simulation results regarding the time-domain waveforms of power factor in three control methods.

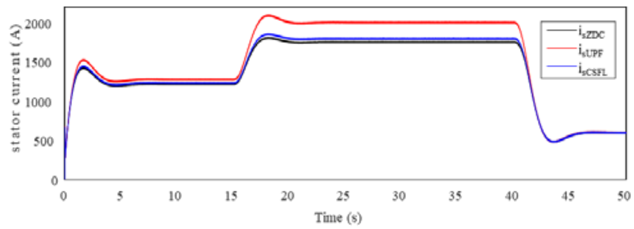

Fig.9 Simulation results regarding the time-domain waveforms with rms stator current in three control methods.

The above analysis can be summarized as shown in Table 3.

TABLE 3: GENERATOR PARAMETERS USED IN SIMULATION

Control methods	***ZDC***	***UPF***	***CSFL***
d-axis stator current	zero	high	middle
q-axis stator current	equal	equal	equal
stator flux	high	low	middle
active power	equal	equal	equal
reactive power	high	zero	middle
apparent power	high	low	middle
power factor	low	1	middle
stator current	low	high	middle
d-axis stator current	zero	high	middle

The summarized Table 3. is shown that

- ZDC control method has poor performance and the reactive power is high therefore the cost is high during wind speed variations.
- UPF control method has high performance during wind speed variations, however, reduce the power rating of the proposed configuration. This would lead to a smaller size and hence reduce the cost of the power circuit, which is one of the significant considerations for megawatt-level wind turbine design.

CSFL control method has approximately high performance and the power factor is approximately one during wind speed variations.

5 Conclusion

This survey could be useful for research on the CSFL control method, which is usually the control method for the motor, is proposed for the control of machine side converter of PMSG in wind turbine based on vector control because it had similar characteristics as ZDC control method and power factor is approximately 1, which is similar characteristics as UPF control method.

Acknowledgment

The authors would like to thank Industrial University of Ho Chi Minh City, Vietnam for providing the funding for this research.

References:

[1] Venkata Yaramasu, Bin Wu, Paresh C. Sen, Samir Kouro, and Mehdi Narimani, High-power wind energy conversion systems: state-of-the-art and emerging technologies. proceeding of the IEEE 2015.

[2] Viktor Perelmuter. Renewable energy systems: Simulation with Simulink and SimPowerSystems, CRC Press Published November 23, 2016.

[3] Mario J. Duran, Federico Barrero, Senior Member, IEEE, Ana Pozo-Ruz, Francisco Guzman, José Fernandez, and Hugo Guzman. "Understanding power electronics and electrical machines in multidisciplinary wind energy conversion system courses", IEEE transactions on education, vol. 56, no. 2, May 2013

[4] Henk Polinder, Jan Abraham Ferreira, Bogi Bech Jensen, Asger B. Abrahamsen, Kais Atallah, Richard A. McMahon, "Trends in wind turbine generator systems" IEEE journal of emerging and selected topics in power electronics, vol. 1, no. 3, September 2013.

[5] Ramji Tiwari, N. Ramesh Babu. "Recent developments of control strategies for wind energy conversion system", Renewable and Sustainable Energy Reviews 66 (2016) 268–285.

[6] Venkata Yaramasu, Apparao Dekka, Mario J. Durán, Samir Kouro, Bin Wu. PMSG - based wind energy conversion systems: survey on power converters and controls. IET Electric Power Appl., 2017, Vol. 11, Iss. 6, pp. 956–968.

[7] Mohsen Rahimi, "Mathematical modeling, dynamic response analysis, and control of PMSG- based wind turbines operating with an alternative control structure in power control mode", Int Trans. Electr. Energ. Syst. 2017; https://doi.org/10.1002/etep.2423.

[8] Hua Ye, Bo Yue, Xuan Li and Kai Strunz. Modeling and simulation of multi - scale transients for PMSG - based wind power systems. Wind Energ. 2017; 20:1349–1364.

[9] Da Xie, Yupu Lu, Junbo Sun, Chenghong Gu. Small signal stability analysis for different types of PMSGs connected to the grid. Renewable Energy 106 (2017) 149-164.

[10] Hua Geng and Dewei (David) Xu. Stability analysis and improvements for variable-Speed multipole permanent magnet synchronous generator-based wind energy conversion system. IEEE transactions on sustainable energy, vol.2, no. 4, October 2011.

[11] Hua Geng, Geng Yang, Dewei (David) Xu, and Bin Wu, Unified power control for PMSG-based WECS operating under different grid conditions. IEEE transactions on energy conversion, vol. 26, no. 3, September 2011.

[12] Youssef Krim, Dhaker Abbes, Saber Krim and Mohamed Faouzi Mimouni. Classical vector, first-order sliding-mode and high-order sliding-mode control for a grid-connected variable-speed wind energy conversion system: A comparative study. Wind Engineering (2017): 1-22.

[13] Haitham Mahmoud Yassin, Hanafy Hassan Hanafy, Mohab M. Hallouda. Enhancement low-voltage ride through capability of permanent magnet synchronous generator - based wind turbines using interval type-2 fuzzy control. IET Renew. Power Gener., 2016, Vol. 10, Iss. 3, pp. 339–348.

[14] Mouna Ben Smida and Anis Sakly. Pitch angle control for grid-connected variable-speed wind turbine system using fuzzy logic: A comparative study. Wind Engineering (2016), pp. 1–12.

[15] E.G. Shehata. A comparative study of current control schemes for a direct-driven PMSG wind energy generation system. Electric Power Systems Research 143 (2017) 197–205.

[16] Marian p. Kazmierkowski, R. Krishnan, Frede Blaabjerg. Control in Power electronics. Academic Press Published 2002.

[17] Shao Zhang, King-Jet Tseng, D. Mahinda Vilathgamuwa, Trong Duy Nguyen, Xiao-Yu Wang. Design of a Robust Grid Interface System for PMSG-Based Wind Turbine Generators. IEEE transactions on industrial electronics, vol. 58, no.1, january 2011.

[18] Abdel-Raheem Youssef, Ahmed I.M. Ali, Mahmoud S.R. Saeed, Essam E.M. Mohamed. Advanced multi-sector P&O maximum power point tracking technique for wind energy conversion system. Electrical Power and Energy Systems 107 (2019) 89–97.